Boundary-Layer Flow of Nanofluids over a Moving Surface in the Presence of Thermal Radiation, Viscous Dissipation and Chemical Reaction

Eshetu Haile
Osmania University

B. Shankar
Osmania University

Recommended Citation

Boundary-Layer Flow of Nanofluids over a Moving Surface in the Presence of Thermal Radiation, Viscous Dissipation and Chemical Reaction

Eshetu Haile[1*] and B. Shankar[2]

Department of Mathematics
Osmania University
Hyderabad 500-007, INDIA
[1]*eshetuhg@gmail.com*; [2]*bandarishanker@yahoo.co.in*

[*]Corresponding Author

Abstract:

The flow problem presented in the paper is boundary-layer flow of nanofluids over a moving surface in the presence of thermal radiation, viscous dissipation and chemical reaction. The plate is assumed to move in the same or opposite direction to the free stream which depends on the sign of the velocity parameter. The partial differential equations appearing in the governing equations are transformed into a couple of nonlinear ordinary differential equations using similarity transformations. The transformed equations in turn are solved numerically by the shooting method along with the fourth order Runge-Kutta integration technique. Influences of the pertinent parameters in the flow field are exhaustively studied and sequentially explained graphically and in tabular form. For selected values of the parameters involved in the governing equations like Lewis number, the velocity parameter, magnetic parameter, Eckert number Brownian motion parameter, thermophoresis parameter, thermal radiation parameter, Prandtl number, Reynolds number and chemical reaction parameter, numerical results for the velocity field, temperature distribution, concentration, skin friction coefficient, Nusselt number and Sherwood number are obtained. The results are analyzed and compared with previously published works; they are found in excellent agreement.

Keywords: Boundary-layer flow, Heat transfer, Mass transfer, Stretching sheet, Nanofluids, Viscous dissipation, Chemical reaction

MSC 2010: 76M20, 76N20, 76W05, 80A20, 35Q35

1. Introduction

Presently, nanofluids are thought to have a wide range benefits in medical application, biomedical industry, detergency, power generation in nuclear reactors and more specifically in any heat removal involved industrial applications. The ongoing research will focus on the

952

Applications and Applied Mathematics: An International Journal (AAM), Vol. 10 [2015], Iss. 2, Art. 21

AAM: Intern. J., Vol. 10, Issue 2 (December 2015)   953

utilization of nanofluids in microelectronics, fuel cells, pharmaceutical processes, hybrid-powered engines, engine cooling, vehicle thermal management, domestic refrigerator, chillers, heat exchanger, nuclear reactor coolant, grinding, machining, space technology, defense and ships, and boiler flue gas temperature reduction as noted by Ahmadreza (2013). It is well known that conventional heat transfer fluids like oil, water and ethylene glycol mixture are poor heat transfer fluids since the thermal conductivity of such fluids play vital roles on the heat transfer coefficient between the heat transfer medium and the heat transfer surface. An innovative technique, which uses a mixture of nanoparticles and the base fluid, was first introduced by Choi (1995) in order to develop advanced heat transfer fluids with substantially higher conductivities. The resulting mixture of the base fluid and nanoparticles having unique physical and chemical properties is referred to as a nanofluid. It is expected that the presence of the nanoparticles in the nanofluid increases the thermal conductivity and therefore substantially enhances the heat transfer characteristics of the nanofluid as explained by Olanrewaju et al. (2012).

Hamad et al. (2011) examined magnetic field effects on free convection flow of a nanofluid past a vertical semi-infinite flat plate. A study on boundary layer flow of a nanofluid past a stretching sheet with a convective boundary condition was conducted by Makinde and Aziz (2011). Olanrewaju et al. (2012) investigated boundary layer flow of nanofluids over a moving surface in a flowing fluid in the presence of radiation. Ahmad et al. (2011) presented a numerical study on the Blasius and Sakiadis problems in nanofluids under isothermal condition. Khan et al. (2012) studied the unsteady free convection boundary layer flow of a nanofluid along a stretching sheet with thermal radiation and viscous dissipation effects in the presence of a magnetic field. Convective flow in porous media has been widely studied in the recent years due to its wide range applications in engineering as investigated in Nield and Bejan (2006), Ingham and Pop (2005) and Vadasz (2008). Bachok et al. (2010) studied on boundary-layer flow of nanofluids over a moving surface in a flowing fluid. Recently, Yohannes and Shanker (2014) investigated melting heat transfer in MHD flow of nanofluids over a permeable exponentially stretching sheet.

Recent developments in hypersonic flights, missile re-entry, rocket combustion chambers, power plants for inter planetary flight and gas cooled nuclear reactors, have focused attention on thermal radiation as a mode of energy transfer, and emphasizes the need for improved understanding of radiative transfer in these processes. When the difference between the surface and the ambient temperature is large, the radiation effect becomes important. Hady et al (2012) studied the flow and heat transfer characteristics of a viscous nanofluid over a nonlinearly stretching sheet in the presence of thermal radiation. Effects of a thin gray fluid on MHD free convective flow near a vertical plate with ramped wall temperature under small magnetic Reynolds number, Rajesh (2010) and free convective oscillatory flow and mass transfer past a porous plate in the presence of radiation of an optically thin fluid, Raptis (2011) have been studied. The presence of thermal radiation for MHD flow, free convection flow, flow through a porous medium and effects on viscoelastic flow have been studied by Rami et al. (2001), Raptis (1998), Chamkha (1997), Khan et al. (2014) and Mohammadein and Amin (2000).

Many applications of MHD boundary layers flow of heat and mass transfer over flat surfaces are found in many engineering and geophysical applications such as geothermal reservoirs, thermal insulation, enhanced oil recovery, packed-bed catalytic reactors, cooling of nuclear reactors.

Bachok et al. (2010) studied boundary layer flow of nanofluids over a moving surface in a flowing fluid. Magnetic field effects on free convection flow of a nanofluid past a vertical semi-infinite flat plate was briefly explained by Hamad et al. (2011). Moreover, MHD flow and heat transfer over stretching/shrinking sheets with external magnetic field, viscous dissipation and joule effects was studied by Jafar et al. (2001). Applications of magnetic field to blood circulation in the human artery systems and its application for the treatment of certain cardiovascular disorders were studied by Gurju et al. (2014). Viscous dissipation changes the temperature distributions by playing a role like energy source, which leads to affect heat transfer rates. The merit of the effect of viscous dissipation depends on whether the sheet is being cooled or heated. Kairi (2011) investigated the effect of viscous dissipation on natural convection in a non-Darcy porous medium saturated with non-Newtonian fluid of variable viscosity; influence of thermal radiation, viscous dissipation and Hall current on MHD convection flow over a stretched vertical flat plate was studied by Redy (2014).

Hadjinicolaou (1993) studied heat transfer in a viscous fluid over a stretching sheet with viscous dissipation and internal heat generation. Steady two dimensional flow of an incompressible viscous and electrically conducting nanofluid caused by a stretching sheet in the vertical direction in the presence of viscous dissipation, which is placed in a saturated porous media has been investigated by Ferdows et al. (2012). On the other hand, transient mixed convective laminar boundary layer flow of an incompressible, viscous dissipative, electrically conducting nanofluid from a continuously stretching permeable surface in the presence of magnetic field and thermal radiation flux has been studied by Ferdows et al. (2013). Recently, many scholars have studied the roles of viscous dissipation and magnetic field in time dependant flows of nanofluids along stretching sheets. Khan et al. (2013) have studied unsteady laminar boundary layer flows of a nanofluid past a stretching sheet with thermal radiation in the presence of magnetic field numerically. Time dependent two dimensional flow of an incompressible viscous and electrically conducting nanofluid induced by a stretching sheet in the vertical direction in a porous medium saturated with quiescent ambient nanofluid has been studied by Beg et al. (2014). They investigated that velocity and momentum boundary layer thickness are enhanced with increasing thermal Grashof number, species Grashof number, Brownian motion parameter and thermophoresis parameter.

In many chemical engineering processes, a chemical reaction between a foreign mass and the fluid does occur. These processes take place in numerous industrial applications, such as the polymer production, the manufacturing of ceramics or glassware, food processing, etc. Khan et al. (2014) studied possessions of chemical reaction on MHD heat and mass transfer nanofluid flow on a continuously moving surface. The role of chemical reaction on heat and mass transfer was studied by Prakash et al. (2014). Kandasamy and Palanimani (2007) studied on effects of chemical reactions, heat and mass transfer on nonlinear magnetohydrodynamic boundary layer flow over a wedge with a porous medium in the presence of ohmic heating and viscous dissipation. Postelnicu (2007) studied the influence of chemical reaction on heat and mass transfer by natural convection from vertical surfaces in porous media considering Soret and Dufour effects.

Since the increasing demand of nanofluids and its applications in science and technology is growing rapidly, a lot has to be done on convective transport of nanofluids. However, boundary-

Applications and Applied Mathematics: An International Journal (AAM), Vol. 10 [2015], Iss. 2, Art. 21

AAM: Intern. J., Vol. 10, Issue 2 (December 2015)   955

layer flow of nanofluids over a moving surface in the presence of thermal radiation, viscous dissipation and chemical reaction are not widely studied in a comprehensive way. Yet, as per my understanding, the simultaneous effects of these parameters together with the boundary conditions on heat and mass transfer flow of nanofluids over a moving flat plate has not been reported. Accordingly, the models and new improvements are presented in this work by extending the works of Olanrewaju et al. (2012) and Motsumi et al. (2012) to include uniform magnetic field, viscous dissipation and chemical reaction in the momentum, energy and concentration equations respectively for more physical implications. The governing boundary layer equations are reduced to a system of highly nonlinear ordinary differential equations using similarity transformations and the resulting equations are solved numerically by using the shooting technique. Influences of various governing parameters on the velocity, temperature and concentration profiles and skin-friction coefficient, Nusselt number and Sherwood number are discussed in detail.

Nomenclature

B Magnetic field strength
C Nanoparticles concentration
C_f Skin friction coefficient
C_w Nanoparticles concentration at the plate
C_∞ Ambient nanoparticles concentration
D_B Brownian motion diffusion coefficient
D_T Thermophoretic diffusion coefficient
Ec Eckert number
f Dimensionless stream function
g Dimensionless temperature
h Dimensionless nanoparticle conc.
Ha Magnetic parameter
k Thermal conductivity of the nanofluid
k^* Rosseland mean absorption coefficient
k_f Thermal conductivity of the base fluid
K_r Chemical reaction parameter
Le Lewis number
Nb Brownian motion parameter
Nt Thermophoretic parameter
Nu_x Local Nusselt number
Pr Prandtl number
R Radiation parameter
Re_x Reynolds's number
Sh_x Local Sherwood number
T Fluid temperature

T_w Temperature at the surface
T_∞ Ambient temperature
U Uniform free stream velocity
u, v Velocity comp. in the x-and y- axes

x; y   Cartesian coordinates measured along and normal to the stretching sheet

Greek Symbols

α Thermal diffusivity of the fluid
λ velocity parameter
σ Electrical conductivity of the base fluid
σ^* Stefan-Boltzmann constant
ψ Stream function
η Dimensionless similarity variable
γ Scaled chemical reaction parameter
μ Dynamic viscosity of the nanofluid
υ Kinematic viscosity of the fluid
ρ_f Density of the base fluid
ρ_p Density of the nanoparticle
τ A parameter defined by $\frac{(\rho C_p)_p}{(\rho C_p)_f}$
$(\rho C_p)_f$ Heat capacity of the base fluid
$(\rho C_p)_p$ Heat capacity of the nanoparticle

E. Haile and B. Shankar

2. Formulation of the Problem

We consider a steady two dimensional MHD boundary layer flow of a nanofluid past a moving semi- infinite flat plate in a uniform free stream in the presence of thermal radiation, chemical reaction and viscous dissipation. We assume that the velocity of the uniform free stream is U and that of the plate is $U_w = \lambda \mathbf{U}$, where λ is the velocity parameter. The flow is assumed to take place at $y \geq 0$, with y being the coordinate measured normal to the moving surface. A variable magnetic field $\mathbf{B}$ is applied in the y direction. It is assumed that the induced magnetic field, the external electric field and the electric field due to the polarization of charges are negligible in comparison to the applied magnetic field. At the moving surface, the temperature and concentration of the nanoparticles take constant values T_w and C_w, respectively. Following these conditions, the governing boundary layer equations of continuity, momentum, energy and diffusion with thermal radiation, viscous dissipation and chemical reaction effects of the nanofluids can be written in Cartesian coordinates x and y in dimensional form as (Olanrewaju et al. (2012) , Bachok et al. (2010), Khan et al. (2014), Stanford and Jagdish (2014)):

$$\frac{\partial u}{\partial x} + \frac{\partial v}{\partial y} = 0 \tag{1}$$

$$u\frac{\partial u}{\partial x} + v\frac{\partial u}{\partial y} = U\frac{dU}{dx} + \frac{\mu}{\rho}\frac{\partial^2 u}{\partial y^2} - \frac{\sigma B^2}{\rho}(u - U), \tag{2}$$

$$u\frac{\partial T}{\partial x} + v\frac{\partial T}{\partial y} = \alpha\frac{\partial^2 T}{\partial y^2} + \frac{\mu}{\rho C_p}\left(\frac{\partial u}{\partial y}\right)^2 - \frac{1}{\rho C_p}\frac{\partial q_r}{\partial y} + \tau\left[D_B\frac{\partial C}{\partial y}\frac{\partial T}{\partial y} + \frac{D_T}{T_\infty}\left(\frac{\partial T}{\partial y}\right)^2\right], \tag{3}$$

$$u\frac{\partial C}{\partial x} + v\frac{\partial C}{\partial y} = D_B\frac{\partial^2 C}{\partial y^2} + \frac{D_T}{T_\infty}\frac{\partial^2 T}{\partial y^2} - K_r(C - C_\infty), \tag{4}$$

where (u, v) are the x and y velocity components, T is temperature, T_∞ and C_∞ are temperature and nanoparticle concentration far from the sheet, respectively; $B = B_0/\sqrt{x}$, B_0 is a constant, σ is the electrical conductivity of the base fluid, ρ_f is density of the base fluid, k_f thermal conductivity of the base fluid and ρ, μ, k and C are the density, dynamic viscosity, thermal conductivity and nanoparticle concentration, ρ_s is the density of the particles, $(\rho C_p)_f$ is the heat capacity of the fluid and $(\rho C_p)_s$ is the effective heat capacity of the nanoparticle material, ν is the kinematic viscosity coefficient, $\alpha = \dfrac{k}{(\rho C_p)_f}$ is the thermal diffusivity of the fluid, q_r is the radiative heat flux, D_B is Brownian diffusion coefficient, D_T is thermophoresis diffusion coefficient, K_r is the chemical reaction parameter and $\tau = \dfrac{(\rho C_p)_p}{(\rho C_p)_f}$.

The boundary conditions associated to the differential equations are:

$$u = U_w = \lambda\mathrm{U}, \ v = 0, \ T = T_w, \ C = C_w \ \text{ at } \ y = 0,$$

$$u \to U, \ T \to T_\infty, \ C \to C_\infty \ \text{ as } \ y \to \infty. \tag{5}$$

Applications and Applied Mathematics: An International Journal (AAM), Vol. 10 [2015], Iss. 2, Art. 21

AAM: Intern. J., Vol. 10, Issue 2 (December 2015) 957

The surface moving parameter $\lambda > 0$ corresponds to the downstream movement of the plate from the origin, while $\lambda < 0$ corresponds to the upstream movement of the plate.

According to the Rosseland diffusion approximation Hossain and Takhar (1996) and following Raptis (1998), the radiative heat flux q_r is given by

$$q_r = -\frac{4\sigma^*}{3k^*}\frac{\partial T^4}{\partial y}, \tag{6}$$

where σ^* and k^* are the Stefan-Boltzmann constant and the Rosseland mean absorption coefficient, respectively. We assume that the temperature differences within the flow are sufficiently small so that T^4 may be expressed as a linear function of temperature

$$T^4 \approx 4T_\infty^3 T - 3T_\infty^4. \tag{7}$$

Using (6) and (7) in Equation (3), we obtain

$$\frac{\partial q_r}{\partial y} = -\frac{16\sigma^* T_\infty^3}{3k^*}\frac{\partial^2 T}{\partial y^2}. \tag{8}$$

In order to reduce the governing equations into a system of ordinary differential equations, we introduce the following local similarity variables:

$$\eta = \left(\frac{U}{2\upsilon x}\right)^{\frac{1}{2}} y, \ T = T_\infty + (T_w - T_\infty)g(\eta), \ C = C_\infty + (C_w - C_\infty)h(\eta),$$
$$\psi = (2U\upsilon x)^{\frac{1}{2}}f(\eta). \tag{9}$$

Here, we introduce the stream function ψ defined as $u = \frac{\partial\psi}{\partial y}$ and $v = -\frac{\partial\psi}{\partial x}$, which identically satisfies Equation (1). Substitution of the similarity variables into Equations (2)-(4) gives:

$$f''' + f f'' - Ha(f' - 1) = 0, \tag{10}$$
$$\left(\frac{3+4R}{3}\right)g'' + Pr\left(fg' + Ecf''^2 + Nbg'h' + Ntg'^2\right) = 0, \tag{11}$$

$$h'' + Lefh' + \frac{Nt}{Nb}g'' - Le.\gamma.Re_x h = 0, \tag{12}$$

where η is the similarity variable, f is the dimensionless stream function, g is dimensionless temperature and h is dimensionless nanoparticles concentration. The corresponding boundary conditions become:

$$f(0) = 0, \ f'(0) = \lambda, \ g(0) = 1, \ h(0) = 1, \tag{13}$$
$$f'(\eta) \to 1, \ g(\eta) \to 0, \ h(\eta) \to 0, \ \text{as } \eta \to \infty.$$

Primes denote differentiation with respect to η, $\gamma = \frac{2vK_r}{U^2}$ (Scaled chemical reaction parameter), $Pr = \frac{v}{\alpha}$ (Prandtl number), $Nt = \frac{(\rho C_p)_s D_T (T_w - T_\infty)}{v(\rho C_p)_f T_\infty}$ (Thermophoresis parameter), $Le = \frac{v}{D_B}$ (Lewis number), $Nb = \frac{(\rho C_p)_s D_B (C_w - C_\infty)}{v(\rho C_p)_f}$ (Brownian motion parameter), $R = \frac{4\sigma^* T_\infty^3}{k^* k}$ (Radiation parameter), $Ec = \frac{U^2}{(C_p)_f (T_w - T_\infty)}$ (Eckert number) and $Ha = \frac{2}{U} \frac{\sigma B_0^2}{\rho_f}$ (Magnetic parameter).

The quantities we interested in studying are the skin-friction coefficient C_f, the local Nusselt number Nu_x and the local Sherwood number Sh_x. These parameters respectively characterize the surface drag, wall heat, and mass transfer rates. The quantities are defined as:

$$C_f = \frac{\tau_w}{\rho U^2}, \qquad Nu_x = \frac{x q_w}{k_f (T_w - T_\infty)}, \qquad Sh_x = \frac{x J_w}{D_B (C_w - C_\infty)} \qquad (14)$$

where τ_w, q_w and J_w are the *shear stress*, *heat flux* and *mass flux* at the surface, respectively and are defined by

$$\tau_w = \mu \left(\frac{\partial u}{\partial y}\right)_{y=0}, \quad q_w = -\left(k + \frac{16\sigma^* T_\infty^3}{3k^*}\right)\left(\frac{\partial T}{\partial y}\right)_{y=0}, \quad J_w = -D_B \left(\frac{\partial C}{\partial y}\right)_{y=0}. \qquad (15)$$

 Using (14) and (15), the dimensionless skin friction coefficient (surface drag), wall heat and mass transfer rates become:

$$\sqrt{2Re_x} C_f = f''(0), \quad \sqrt{\frac{2}{Re_x}} Nu_x \frac{k_f}{k} = -\left(\frac{3+4R}{3}\right) g'(0) \quad \text{and} \quad \sqrt{\frac{2}{Re_x}} Sh_x = -h'(0), \qquad (16)$$

where $Re_x = \frac{xU}{v_f}$ is the local Reynolds number. According to Bachok et al. (2010), $\frac{Nu_x}{\sqrt{Re_x}}$ and $\frac{Sh_x}{\sqrt{Re_x}}$ are referred to as the reduced Nusselt number and reduced Sherwood numbers which are represented by $-g'(0)$ and $-h'(0)$, respectively.

3. Numerical solution

Since Equations (10)-(12) are non-linear ODEs, it is impossible to find the closed form solutions. Thus, these equations with the boundary conditions (13) are solved numerically using the shooting technique along with the fourth order Runge-Kutta integration scheme.

The boundary value problem is converted to an initial value problem as shown below:

$$\text{Let } f = f_1, \ f_1' = f_2, f'_2 = f_3, \text{ then } f''' = f'_3 = -f_1 f_3 + Ha(f_2 - 1); \qquad (17)$$

$$g = f_4, \ g' = f_5, \text{ then } f'_5 = g'' = \frac{-3Pr}{3+4R}(f_1 f_5 + Ec(f_3)^2 + Nb f_5 f_7 + Nt(f_5)^2), \qquad (18)$$

and

Applications and Applied Mathematics: An International Journal (AAM), Vol. 10 [2015], Iss. 2, Art. 21

AAM: Intern. J., Vol. 10, Issue 2 (December 2015)   959

$$h = f_6, \; h' = f_7,$$

which results in

$$h'' = -Le.f_1 f_7 + \frac{3PrNt}{Nb(3+4R)}(f_1 f_5 + Ec(f_3)^2 + Nb.f_5 f_7 + Nt(f_5)^2) + Le.\gamma.Rex.f_6, \qquad (19)$$

with the boundary conditions

$$f_1(0) = 0, \; f_2(0) = \lambda, \; f_4(0) = 1, \; f_6(0) = 1, \; f_2(\infty) = 1, \; f_4(\infty) = 0, \; f_6(\infty) = 0. \qquad (20)$$

Table1: *Comparison of $f''(0)$, $-g'(0)$ and $-h'(0)$ for various values of Pr, Nb, Nt, Le, R and λ when $Ec = Ha = \gamma = 0$.*

| Parameters						$f''(0)$		$-g'(0)$		$-h'(0)$	
Pr	Nb	Nt	Le	R	λ	Olanrewaju (2012)	Present Work	Olanrewaju (2012)	Present Work	Olanrewaju (2012)	Present Work
0.71	0.1	0.1	2	2	0.1	0.462512	0.462512	0.263891	0.263891	0.630473	0.630473
0.71	0.1	0.1	2	4	0.1	0.462512	0.462512	0.213218	0.213218	0.644033	0.644033
0.71	0.1	0.1	2	1	2	-1.01906	-1.019061	0.509487	0.509487	1.325517	1.325517
1	0.1	0.1	2	1	0.1	0.462512	0.462512	0.353009	0.353010	0.600376	0.600376
2	0.5	0.5	2	1	0.1	----------	0.462512	0.308307	0.308307	0.662384	0.662384
2	0.5	0.5	2	1	1.5	----------	-0.45778	0.536323	0.536323	1.196426	1.196426
2	0.5	0.5	6	1	1	----------	0.000000	----------	0.434794	1.955457	1.955457
2	0.5	0.5	10	1	0.1	----------	0.462512	----------	0.282348	1.295602	1.295602

In order to integrate (17), (18) and (19) as an initial value problem, we require values for $f_3(0) := p$, $f_5(0) := q$ and $f_7(0) := r$ that is $f''(0)$, $g'(0)$ and $h'(0)$, respectively. Such values are not given in the boundary conditions (20). These values are what we are striving to find in our paper for various values of the physical parameters.

The most important task of shooting method is to choose the appropriate finite values of η_∞. In order to determine η_∞ for the boundary value problem stated by Equations (17)-(20), we start with some initial guess values for some particular set of physical parameters to obtain $f''(0)$, $g'(0)$ and $h'(0)$ differ by pre-assigned significant digit. The last value of η_∞ is finally chosen to be the most appropriate value of the limit η_∞ for that particular set of parameters. The value of η_∞ may change for another set of physical parameters. Once the finite value of η_∞ is determined, then the integration is carried out as stated by Mandal and Mukhopadhyay (1996). Accordingly, the initial condition vector for the boundary value problem is given by $[f(0), f'(0), f''(0), g(0), g'(0), h(0), h'(0)]$ that is $Y_0 = [0, \lambda, p, 1, q, 1, r]$.

We took the series of values for $f''(0)$, $g'(0)$ and $h'(0)$ and applied the fourth order Runge – Kutta integration scheme with step size $h = 0.01$. The above procedure was repeatedly performed till we obtained the desired degree of accuracy, 10^{-6}. With the help of the Matlab software, the desired results are generated, the graphs are sketched and their interpretations are given as shown in the coming section.

4. Results and Discussion

In the numerical solutions, effects of magnetic field, viscous dissipation, thermal radiation and chemical reaction on heat and mass transfer characteristics of a moving plate of nanofluids were considered. The transformed nonlinear ordinary differential equations (10)–(12) subject to the boundary conditions (13) were solved numerically using the shooting technique followed by the classical fourth order Runge–Kutta method.
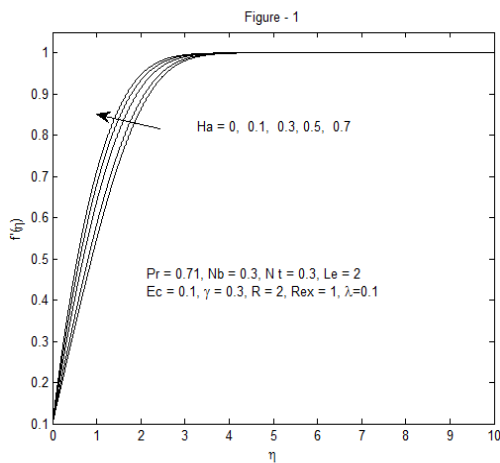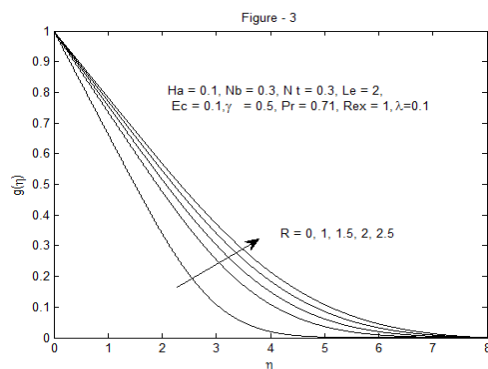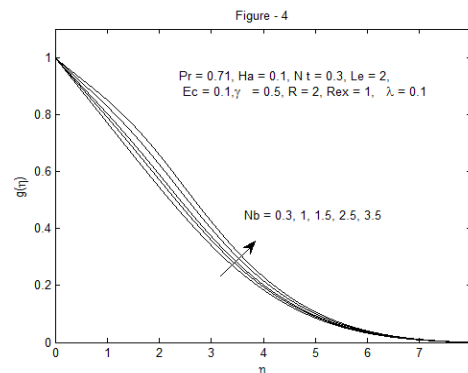

Figure 1. Effects of Ha on velocity profile
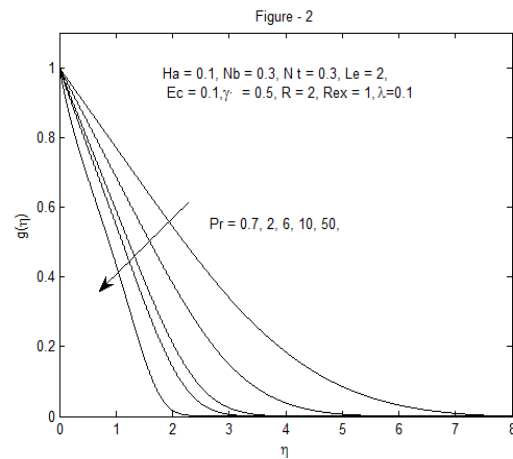
Figure 2. Effects of Pr on temp. profile

Velocity, temperature and concentration profiles were obtained and we applied the results to compute the skin friction coefficient, the local Nusselt and local Sherwood numbers. The numerical results were discussed for the various values of the embedded parameters graphically and in table form. To validate the accuracy of the numerical results, comparisons were made
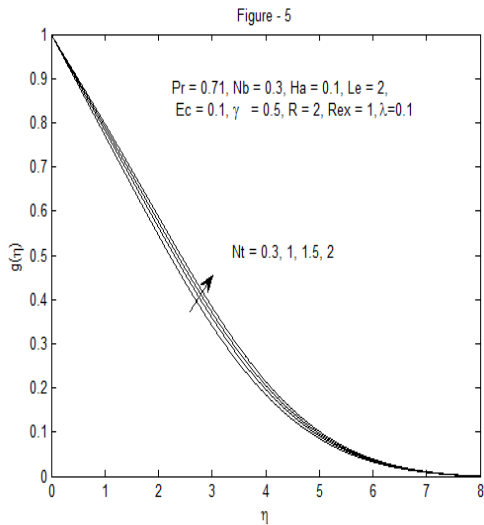

Figure 3. Effects of R on temp. profile

Figure 4. Effects of Nb on temp. profile

Applications and Applied Mathematics: An International Journal (AAM), Vol. 10 [2015], Iss. 2, Art. 21

AAM: Intern. J., Vol. 10, Issue 2 (December 2015) 961

with Olanrewaju et al. (2012) in the absence of viscous dissipation, magnetic field and chemical reaction; as shown in Table1, the results are in good agreement and so the validity of our method is ensured.
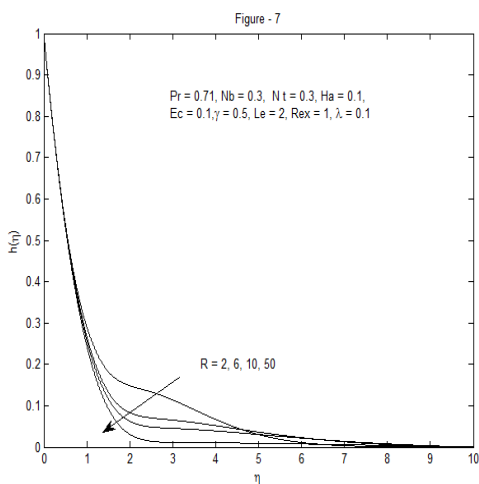

Figure 5. Effects of Nt on temp. profile
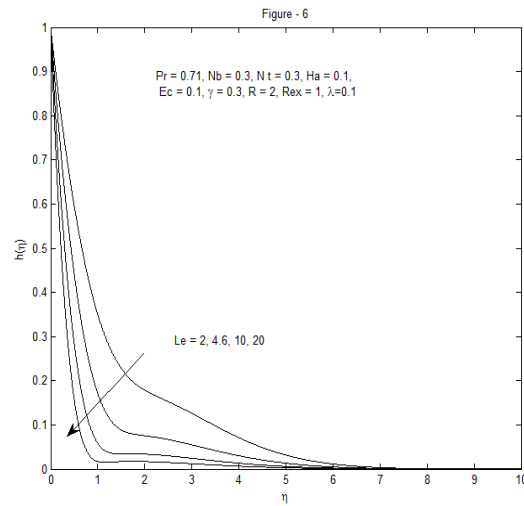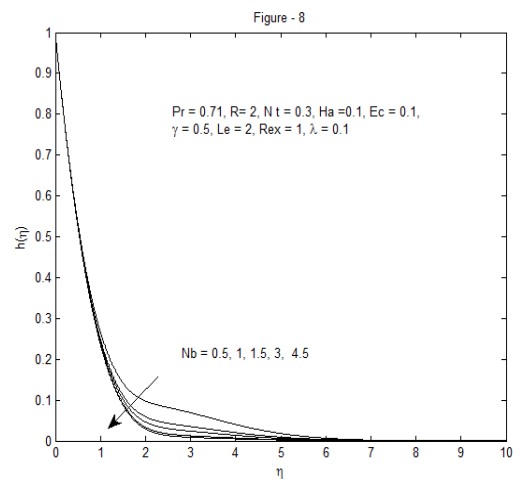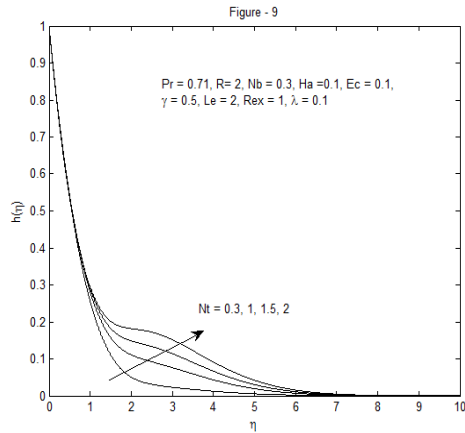

Figure 6. Effects of Le on conc. profile

The skin friction coefficient, wall heat and mass transfer rates for different values of $Pr, Nb, Nt,$ λ, R and Le are given in Table1 when $Ec = Ha = \gamma = 0$. For some prescribed values of $Ec, Ha,$ γ and Re_x together with the other embedded parameters and numbers, some fluid dynamic quantities were presented. For clarity, let us see the effects of parameters like Brownian motion, thermophoresis, viscous dissipation, thermal radiation, scaled chemical reaction and Lewis number, magnetic parameter, Prandtl number and Eckert number on various fluid dynamic quantities as presented graphically and in tabular form.
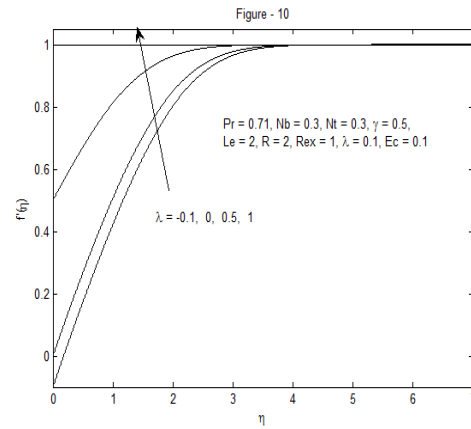

Figure 7. Effects of R on conc. profile
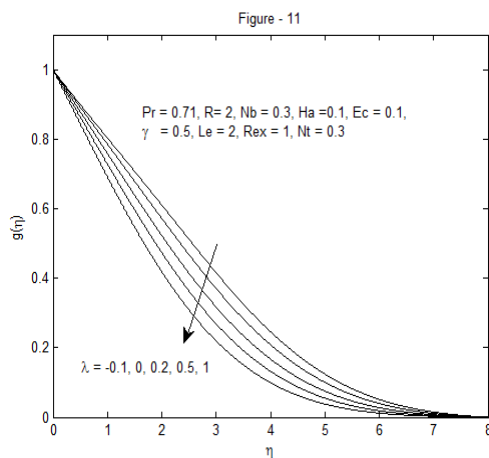

Figure 8. Effects of Nb on conc. profile
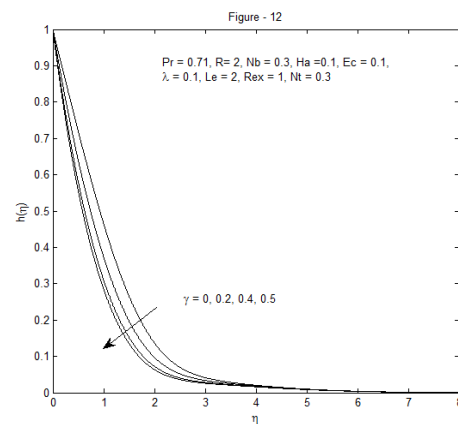
Figure 9. Effects of Nt on conc. profile

Figure 10. Effects of λ on velocity profile

The effect of magnetic field parameter Ha on velocity profile $f'(\eta)$ is pictured in Figure1. The essence of the magnetic parameter has been explained from the sign of the term $\frac{\sigma B^2}{\rho}(u - U)$ in Equation (2). This term is composed of the imposed pressure force $\frac{\sigma B^2}{\rho}U$ and the Lorentz force $\frac{\sigma B^2}{\rho}u$, which slows down the fluid motion in the boundary layer region. When the imposed pressure force overcomes the Lorentz force $(U > u)$, the effect of the magnetic parameter increases the velocity. Similarly, when the Lorentz force dominates the imposed pressure force $(u > U)$, the effect of the magnetic parameter decreases velocity flow and hence it decreases momentum boundary layer thickness (Rana and Anwar (2014)).

Figure 2 shows the effect of Prandtl number Pr on temperature profile. As Pr increases, the temperature profile decreases. Figure 3 shows the effect of thermal radiation parameter R on temperature profile. As R increases, the temperature profile also increases.
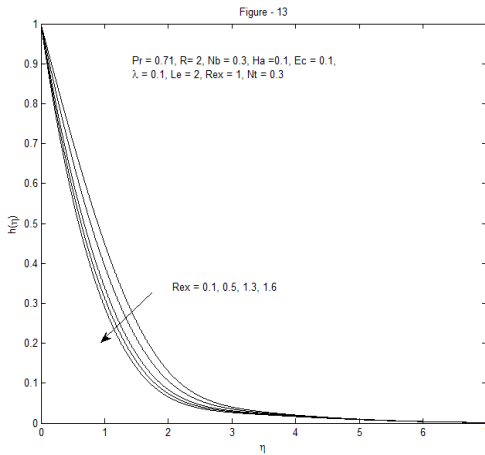

Figure 11. Effects of λ on temp. profile

**Figure 12.** Effects of γ on conc. profile

Applications and Applied Mathematics: An International Journal (AAM), Vol. 10 [2015], Iss. 2, Art. 21

AAM: Intern. J., Vol. 10, Issue 2 (December 2015)   963

Figure 4 shows the effect of Brownian motion parameter Nb on temperature profile. As shown in the figure, the Brownian motion parameter enhances the temperature profile.
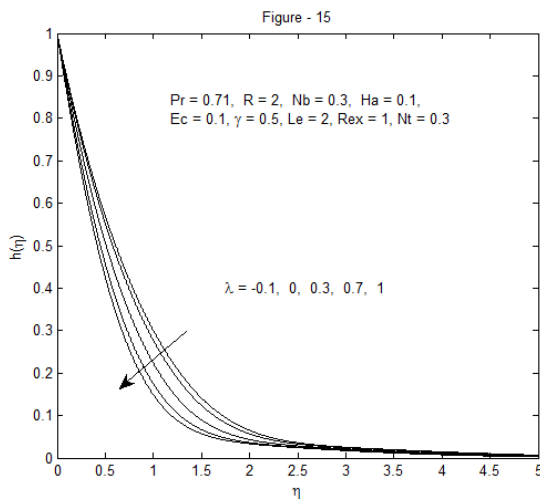

Figure 13. Effects of Re_x on conc. profile
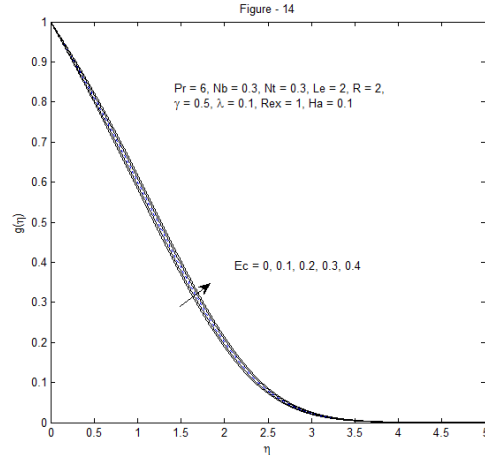
Figure 14. Effects of Ec on temp. profile

Figure 5 and Figure 9 show the effect of thermophoresis parameter Nt on temperature and concentration profiles. As the thermophoresis parameter increases, both the temperature and concentration profiles also increase. Figure 6 illustrates the effect of Lewis number on concentration. It is clearly shown in the figure that as the Lewis number increases, the concentration profile decreases significantly. This is because the increment of Lewis number reduces Brownian diffusion coefficient D_B and this leads the flow to decline the concentration profile. This is obvious from the very definition of the parameter.

Figure 7 shows the effect of thermal radiation parameter R on concentration profile. As R increases, the concentration profile decreases. Figure 8 illustrates the effect of Brownian motion parameter Nb on concentration profile. It is clearly illustrated that as Nb increases, the concentration profile decreases.

Figure 15. Effects of λ on conc. profile
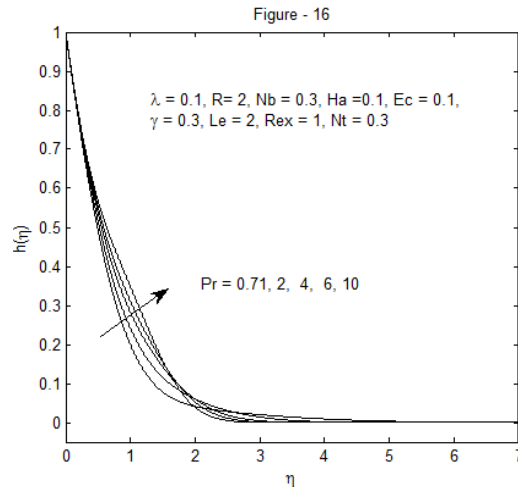
Figure 16. Effects of Pr on conc. profile

Figures.10, 11 and 15 show effects of the velocity parameter λ on velocity, temperature and concentration profiles. For a fixed value of η, as the parameter λ increases, the velocity profile also increases and finally it is getting constant as λ is closer to 1. On the other hand, the parameter reduces both the temperature and concentration profiles considerably.

Table 2: Comparison of $f''(0)$, $-g'(0)$ and $-h'(0)$ on themselves for various values of Le and Re_x

For $Nt = 0.3$, $Pr = 6$, $Le = 2$, $Nb = 0.3$, $Ec = 0.1$, $\gamma = 0.3$, $Ha = 0.1$, $R = 2$, $Re_x = 1$, $\lambda = 0.1$							
Le	$f''(0)$	$-g'(0)$	$-h'(0)$	Re_x	$f''(0)$	$-g'(0)$	$-h'(0)$
2	0.537052	0.355109	1.023657	0.5	0.537052	0.361494	0.859500
6	0.537052	0.326789	1.716981	1	0.537052	0.355109	1.023657
10	0.537052	0.317791	2.162991	1.3	0.537052	0.351883	1.112757
20	0.537052	0.308813	2.960850	1.5	0.537052	0.349936	1.168915
50	0.537052	0.301027	4.517598	1.6	0.537052	0.349016	1.196119

Figure 12 shows the effect of chemical reaction parameter γ on concentration profile. Chemical reaction parameter reduces the concentration profile. This is true because as chemical reaction takes place, the amount of nanoparticles within the fluid is getting smaller and smaller. Figure13 also shows the effect of local Reynolds number Re_x on concentration profile. As the Reynolds number increases, the concentration profile decreases.

Figure14 shows the effect of viscous dissipation parameter Ec on temperature profile. As shown in the figure, temperature profile increases with increasing values of viscous dissipation parameter Ec. Figure16 shows the effect of Prandtl number on concentration profile. As the parameter increases near the boundary layer, the concentration profile also increases. But as η gets larger, the opposite happens with slower rate.

Table 2 shows the effect of Lewis number and Reynolds number on skin friction coefficient $f''(0)$, wall heat transfer rate $-g'(0)$ and wall mass transfer rate $-h'(0)$. As it is clearly described, none of these numbers has effects on skin friction coefficient. However, as the Lewis number increases, heat transfer rate decreases while mass transfer rate increases continuously. On the other hand, as the Reynolds number increase, mass transfer rate also increases but heat transfer rate decreases.

Table 3 shows the effect of magnetic parameter and Eckert number on skin friction coefficient, wall heat transfer and wall mass transfer rates. We obtained that viscous dissipation parameter Ec has no effect on the skin friction coefficient $f''(0)$ whereas the magnetic parameter Ha enhances the skin friction coefficient, heat and mass transfer rates. It is clearly described that as the Eckert number increases, heat transfer rate $-g'(0)$ decreases while the opposite is true for mass transfer rate $-h'(0)$. This is true because as the values of both magnetic parameter and viscous dissipation parameters increase, the thermal boundary layer thickness increases. This results in a decline of the wall heat transfer rate.

Applications and Applied Mathematics: An International Journal (AAM), Vol. 10 [2015], Iss. 2, Art. 21

AAM: Intern. J., Vol. 10, Issue 2 (December 2015)   965

Table 3: Comparison of $f''(0)$, $-g'(0)$ and $-h'(0)$ on themselves for various values of Ha and Ec

For $Nt = 0.3$, $Pr = 6$, $Le = 2$, $Nb = 0.3$, $Ec = 0.1$, $\gamma = 0.3$, $Ha = 0.1$, $R = 2$, $Re_x = 1$							
Ha	$f''(0)$	$-g'(0)$	$-h'(0)$	Ec	$f''(0)$	$-g'(0)$	$-h'(0)$
0.0	0.462512	0.349121	1.012449	0	0.537052	0.383582	1.003374
0.05	0.500954	0.352333	1.018275	0.1	0.537052	0.355109	1.023657
0.1	0.537052	0.355109	1.023657	0.2	0.537052	0.326555	1.044005
0.15	0.571181	0.357535	1.028671	0.3	0.537052	0.297917	1.064419
0.2	0.603626	0.359672	1.033373	0.5	0.537052	0.240393	1.105446

Figure 17(a) and Figure 17(b) show the wall heat transfer rate, $-g'(0)$ and the wall mass transfer rate, $-h'(0)$ respectively, as functions of the velocity parameter λ for different values of the radiation parameter R. It is observed that $-g'(0)$ is a decreasing function of the radiation parameter R but it increases with λ while $-h'(0)$ is an increasing function of both the velocity parameter λ and the thermal radiation parameter R.

(a) Heat Transfer Rate   **(b) Mass Transfer Rate**
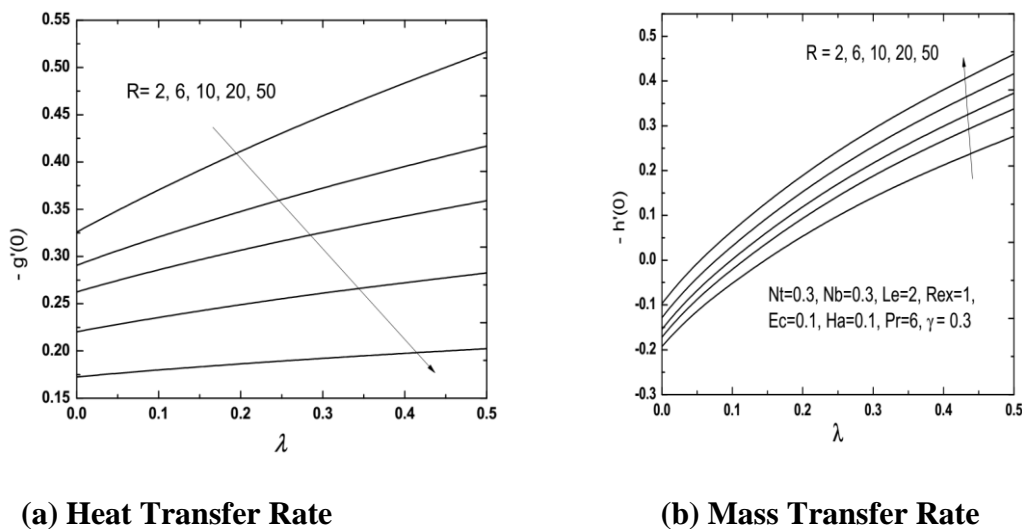
Figure 17. Effects of R and λ on (a) and (b) when $Pr = 6$, $Nb = 0.3$, $Nt = 0.3$, $Ec = 0.1$, $Le = 2$, $Ha = 0.1$, $\gamma = 0.3$, $Re_x = 1$

Effects of Prandtl number Pr and chemical reaction parameter γ on the wall heat and mass transfer rates are shown in Figures 18 (a) and (b). Smaller values of Prandtl number enhances the wall heat transfer rate; the parameter also assists in maximizing the wall mass transfer rate. As expected, the chemical reaction parameter strongly enhances the wall mass transfer rate but its effect to heat transfer rate is minimal for smaller values of Prandtl number. We noticed some irregularities near the boundary layer when the Prandtl number gets larger. It is observed that when the Prandtl number becomes larger, the rate of heat transfer increases near the boundary layer and declines very fast far away from the boundary.

(a) Heat Transfer Rate   **(b) Mass Transfer Rate**
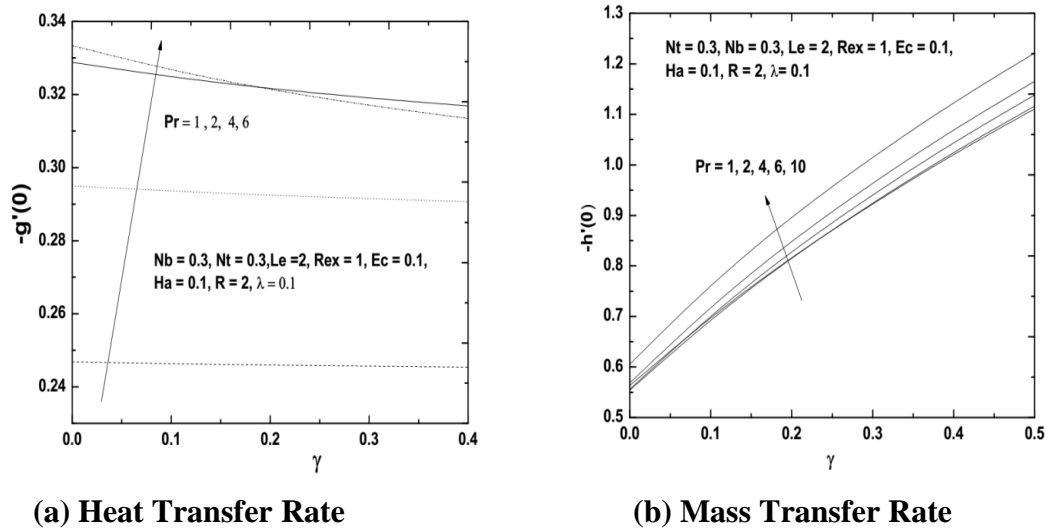
Figure18: Effects of Pr and γ on (a) and (b) when $R = 2, \mathrm{Nb} = 0.3, \mathrm{Nt} = 0.3,\ \mathrm{Ec} = 0.1,$
$Re_x = 1,\ \mathrm{Le} = 2,\ \mathrm{Ha} = 0.1, \lambda = 0.1$

Effects of Brownian motion and thermophoresis parameters on the skin friction coefficient, wall heat and mass transfer rates are shown in Table 4. The table depicts that neither the Brownian nor the thermophoresis parameter has effect on the skin friction coefficient. Nevertheless, as these parameters increase the heat transfer rate reduces significantly; on the other hand, the Brownian motion parameter brings no significant change on the mass transfer rate. Thermophoresis parameter enhances the mass transfer rate.

Table 4: Comparison of $f''(0)$, $-g'(0)$ and $-h'(0)$ on themselves for various values of Nb and Nt

For $Nt = 0.3,\ Pr = 6,\ Le = 2,\ Nb = 0.3, Ec = 0.1,\ \gamma = 0.3,\ Ha = 0.1,\ R = 2,\ Re_x = 1,\ \lambda = 0.1$							
Nb	$f''(0)$	$-g'(0)$	$-h'(0)$	Nt	$f''(0)$	$-g'(0)$	$-h'(0)$
0.5	0.537052	0.283771	1.039093	0.2	0.537052	0.381194	1.000813
1	0.537052	0.154922	1.037616	0.5	0.537052	0.308652	1.093274
2	0.537052	0.036563	1.019768	0.75	0.537052	0.259896	1.211334
2.5	0.537052	0.014261	1.013037	1	0.537052	0.219754	1.348803
3.5	0.537052	0.002137	1.004158	1.5	0.537052	0.159288	1.639565

5. Conclusions

The problem of heat and mass transfer of MHD flow of nanofluids in the presence of viscous dissipation, thermal radiation and chemical reaction effects has been analyzed. The non-linear governing equations associated with the boundary conditions were transformed into a two-point non-linear coupled ODEs with the help of similarity transformation equations. The solutions of these problems were numerically solved with the help of the shooting technique followed by the

Applications and Applied Mathematics: An International Journal (AAM), Vol. 10 [2015], Iss. 2, Art. 21

AAM: Intern. J., Vol. 10, Issue 2 (December 2015)   967

classical fourth order Runge-Kutta method. Among the many significant results, some of them are listed below:

- The velocity profile increases with increasing values of both magnetic and velocity parameters.
- Viscous dissipation, thermal radiation, Brownian motion and thermophoresis parameters enhance the temperature profile whereas Prandtl number and the velocity parameter λ reduce it significantly.
- Thermophoresis parameter enhances the concentration profile; on the other hand, Reynolds number, Lewis number, radiation parameter, Brownian motion parameter, chemical reaction parameter and velocity parameter reduce the concentration profile.
- Magnetic parameter enhances skin friction coefficient, heat and mass transfer rates at the plate surface.
- The presence of Lewis number, Reynolds number, thermal radiation, thermophoresis, velocity, Brownian motion and viscous dissipation parameters in the flow field reduces the rate of thermal boundary layer thickness whereas Prandtl number maximizes the rate of thermal boundary layer thickness.
- The wall mass transfer rate is an increasing function of Lewis number, Prandtl number, Reynolds number, thermophoresis, chemical reaction, radiation, velocity and viscous dissipation parameters whereas Brownian motion parameter reduces mass transfer rate at the plate surface.

Acknowledgement

REFERENCES

Ahmad, S., Rohni, A. M. and Pop, I. (2011). Blasius and Sakiadis problems in nanofluids, Acta Mechanical, vol. 218.

Ahmadreza, A. B. (2013). Application of nanofluid for heat transfer enhancement, PID: 2739168, EEE-5425.

Bachok, N., Ishak, A. and Pop, I. (2010). Boundary layer flow of nanofluids over a moving surface in a flowing fluid, Int. J. of Thermal Sci., vol. 49.

Be´g, O. A, Khan, M.S., Karim, I., Alam, Md. M., Ferdows, M. (2013). Explicit numerical study of unsteady hydromagnetic mixed convective nanofluid flow from an exponentially stretching sheet in porous media, Applied Nanoscience, vol. 2014(3), DOI 10.1007/s13204-013-0275-0.

Chamkha, A. J. (1997). Solar radiation assisted convection in uniform porous medium supported by a vertical plate, Transaction ASME J. of Heat Trans., vol.119.

Choi, S. U. (1995). Enhancing thermal conductivity of fluids with nanoparticles, Developments and App. of Non-Newtonian Flows FED, vol. 66.

Ferdows, M., Khan, M. S., Alam, M. M. and Sun, S. (2012). MHD mixed convective boundary layer flow of a nanofluid through a porous medium due to an exponentially stretching sheet, Mathematical Problems in Engineering, vol. 2012, ID 408528.

Ferdows, M., Khan, M. S., Bég, O. A., Azad, MAK and Alam, M. M. (2013). Numerical study of transient magnetohydrodynamic radiative free convection nanofluid flow from a stretching permeable surface, Proceedings of the Institution of Mechanical Engineers, Part E: Journal of Process Mechanical Engineering, DOI: 10.1177/0954408913493406.

Gurju, A., Radhakrishnamacharya, G. and Shireesha, B. (2014). Effect of slip condition on couple stress fluid flow in a channel with mild Stenosis in the presence of uniform magnetic field, Applications and Applied Mathematics, vol. 9, No. 1.

Hadjinicolaou, K. (1993). Heat transfer in a viscous fluid over a stretching sheet with viscous dissipation and internal heat generation, Int. Comm. in Heat and Mass Tran., vol. 20.

Hady, F. M., Ibrahim, F., Abdel-Gaied, S. S. M. and Eid Mohamed, R. (2012). Radiation effect on viscous flow of a nanofluid and heat transfer over a nonlinearly stretching sheet, Nanoscale Res Lett., vol. 7, http://www.nanoscalereslett.com/content/7/1/229.

Hamad, M. A. Pop, I. and Md. Ismail, A. I. (2011). Magnetic field effects on free convection flow of a nanofluid past a vertical semi-infinite flat plate, Nonlinear Analysis: Real World Appl., vol.12.

Hossain, M. A. and Takhar, H. S. (1996). Radiation effect on mixed convection along a vertical plate with uniform surface temperature, Heat Mass Tran., vol. 31.

Ingham, D. B. and Pop, I. (2005). Transport Phenomena in Porous Media, Elsevier; Oxford Vol. III.

Jafar, K., Nazar, R., Ishak, A. and Pop, I. (2001). MHD flow and heat transfer over stretching or shrinking sheets with external magnetic field, viscous dissipation and Joule effects, Canadian J. Chem. Eng., vol. 9999.

Kairi, R. R. (2011). Effect of viscous dissipation on natural convection in a non-Darcy porous medium Saturated with Non-Newtonian Fluid of Variable Viscosity, The Open Transport Phenomena, vol. 3.

Kandasamy, R. and Palanimani, P. G. (2007). Effects of chemical reactions, heat and mass transfer on nonlinear magnetohydrodynamic boundary layer flow over a wedge with a porous medium in the presence of ohmic heating and viscous dissipation, J. of Porous Media, vol.10.

Khan, M.S., Alam, M.M. and Ferdows, M. (2013). Effects of magnetic field on radiative flow of a nanofluid past a stretching sheet, Procedia Engineering, vol. 56.

Khan, M. S., Karim, I., Ali, L. E. and Islam, A. (2012). Unsteady MHD free convection boundary-layer flow of a nanofluid along a stretching sheet with thermal radiation and viscous dissipation effects, Int. Nano Lett., vol. 2, No. 24, doi:10.1186/2228-5326-2-24.

Khan, M.S., Karim, I., Islam, M.S. and Wahiduzzaman, M. (2014). MHD boundary layer radiative, heat generating and chemical reacting flow past a wedge moving in a nanofluid, Nano Convergence, vol.1, No. 1.

Khan, Md S., Karim, I. and Islam, Md S. (2014). Possessions of chemical reaction on MHD heat and mass transfer nanofluid flow on a continuously moving surface, American Chem. Sci. J., vol. 4, No. 3.

Applications and Applied Mathematics: An International Journal (AAM), Vol. 10 [2015], Iss. 2, Art. 21

AAM: Intern. J., Vol. 10, Issue 2 (December 2015)   969

Makinde, O. D. and Aziz, A. (2011). Boundary layer flow of a nanofluid past a stretching sheet with a convective boundary condition, Int. J. of Thermal Sci., vol. 50.

Mandal, I. C. and Mukhopadhyay, S. (2013). Heat transfer analysis for fluid flow over an exponentially stretching porous sheet with surface heat flux in porous medium, Ain Shams Eng. J., vol. 4, No. 1.

Mohammadein, A. A. and El-Amin, M. F. (2000). Thermal radiation effect on power law fluid over a Horizontal plate embedded in a porous medium, Int. Comm. in Heat and Mass Tran., vol. 27.

Motsumi, T. G. and Makinde, O. D. (2012). Effects of thermal radiation and viscous dissipation on boundary layer flow of nanofluids over a permeable moving flat plate, Physics Scr., vol. 86.

Nield, D. A. and Bejan, A. (2006). Convection in Porous Media, Third ed, Springer; New York.

Olanrewaju, P. O., Olanrewaju, M. A. and Adesanya, A. O. (2012). Boundary layer flow of nanofluids over a moving surface in a flowing fluid in the presence of radiation, Int. J. of App. Sci. and Tech., vol. 2, No. 1.

Postelnicu, A. (2007). Influence of chemical reaction on heat and mass transfer by natural convection from vertical surfaces in porous media considering Soret and Dufour effects, Heat Mass Trans., vol. 43.

Prakash, J., Vijaya Kumar, A. G., Madhavi, M. and Varma, S. V. K. (2014). Effects of chemical reaction and radiation absorption on MHD flow of dusty viscoelastic fluid, Applications and Applied Mathematics, vol. 9, No. 1.

Rajesh, V. (2010). Radiation effects on MHD free convective flow near a vertical plate with ramped wall temperature, Int. J. of App. Math. and Mech., vol. 6, No. 21.

Rami, Y. Jumah, Fawzi, A. Banat and Fahmi Abu-Al-Rub (2001). Darcy-Forchheimer mixed convection heat and mass transfer in fluid saturated porous media, Int. J. of Num. Meth. for Heat and Fluid Flow, vol. 11, No. 6.

Rana, P. and Anwar Be´g, O. (2014). Mixed convection flow along an inclined permeable plate: effect of magnetic field, nanolayer conductivity and nanoparticle diameter, Appl Nanosci, DOI 10.1007/s13204-014-0352-z.

Raptis, A. (1998). Radiation and free convection flow through a porous medium, Int. Comm. in Heat and Mass Trans., vol. 25.

Raptis, A. (2011). Free convective oscillatory flow and mass transfer past a porous plate in the presence of radiation for an optically thin fluid, Thermal Sci., vol.15, No. 3.

Reddy, G. (2014). Influence of thermal radiation, viscous dissipation and Hall current on MHD convection flow over a stretched vertical flat plate, Ain Shams Eng. J., vol. 5.

Stanford, S. and Jagdish, P. (2014). A new numerical approach for MHD laminar boundary layer flow and heat transfer of nanofluids over a moving surface in the presence of thermal radiation, Shateyi and Prakash Boundary Value Problems, vol. 2014(2).

Vadasz, P. (2008). Emerging topics in heat and mass transfer in porous media, Springer; New York.

Yohannes, Y. and Shankar, B. (2014). Melting heat transfer in MHD flow of nanofluids over a permeable exponentially stretching sheet, J. of Nanofluids, vol. 3.